Journal of Hazardous Materials 187 (2011) 401–406

Contents lists available at ScienceDirect

Journal of Hazardous Materials

journal homepage: www.elsevier.com/locate/jhazmat

Sequestration of cadmium ions using titanate nanotube

Alan J. Du[a], Darren D. Sun[a,*], James O. Leckie[b]

[a] School of Civil and Environmental Engineering, Nanyang Technological University, 50 Nanyang Avenue, Singapore 639798, Republic of Singapore
[b] Department of Civil and Environmental Engineering, Stanford University, Stanford, CA 94305, USA

ARTICLE INFO

Article history:
Received 12 October 2010
Received in revised form
27 December 2010
Accepted 11 January 2011
Available online 18 January 2011

Keywords:
Titanate
Cadmium
Sorption
CDMUSIC
Ionic strength

ABSTRACT

In this manuscript, titanate ($Na_2Ti_3O_7$) nanotubes synthesized from alkali hydrothermal route, with high BET surface area (206 m^2/g), were used as an effective sorbent to remove cadmium ions from water. Sorption capacity ($q_{m,Langmuir}$ = 1.1 mmol/g at pH 7) was higher than other sorbents. X-ray photoelectron spectroscopy (XPS) analyses performed on fresh and cadmium-sorbed samples reveal intensities of Na 1s peak decreased after sorption indicating ion-exchanging between cadmium and sodium ions occurred at interlayer of nanotubes. However kinetic study did not show a stoichiometrically equivalent amount of Na^+ being released suggesting Cd uptake was not due solely to ion-exchange mechanism. Batch tests also showed that cadmium uptake was not significantly affected by variation in ionic strength, signifying cadmium ions form an inner-sphere complexation with surface hydroxyl groups. Finally, surface complexation modeling was performed based on charge distribution multisite ion complexation (CDMUSIC) model. It was found that CDMUSIC was able to fit the experimental data best when inner-sphere complexation and ion-exchange were applied together.

1. Introduction

Cadmium is a toxic heavy metal and a possible carcinogen to humans. Anthropogenic origins of cadmium include wastewater of many industries such as pigments, batteries, pesticides, plastics manufacturing and metal-plating. Due to the inability to biologically remove the element, cadmium is accumulated inside the human body. Prolonged exposure to the heavy metal can result in cancer and other chronic illnesses [1–3].

Treatment methods to separate heavy metals from the wastewater include coagulation–precipitation, sorption, electrolysis and nanofiltration. Despite emerging technologies, sorption remains a cost-effective and widely studied method for the removal of heavy metals from water [4–6]. Recently, inorganic titanate nanotubes have received increasing attention as a sorbent for removal of various pollutants. The monocrystalline titanate nanotube has high surface area and dimensions comparable to that of multiwalled carbon nanotube. The morphology of nanotube also allows itself to have better separation/recovery efficiency than nanoparticle. Studies have shown that the one-dimensional materials can be efficiently separated by membrane filtration [7]. Similar to TiO_2 anatase and rutile, titanate nanotube is resilient under acid and basic conditions. Clearly, the aforementioned characteristics would make titanate nanotube a potential sorbent.

Sun and Li [8] studied the uptake of six cations by titanate nanotubes. Ou et al. [9] applied titanate nanotube to sorb aqueous ammonium species. Niu et al. [10] investigated the feasibility of titanate nanotubes as sorbents for arsenic removal. Liu et al. [11] used titanate nanotube for the removal of copper (II) ions from water. From the mentioned literatures, the sorption mechanism was either attributed exclusively to the ion-exchange at the interlayer of the nanotube or not stated at all. However, in surface chemistry metal oxides are known to have hydroxyl groups at its solid–water interface and these functional groups are capable of adsorbing protons and other ions from the bulk solution.

In view of the handful of inconclusive studies, there is need for more in-depth analyses on sorption of ions onto titanate nanotube. Hence the objectives of this work are to (i) synthesize titanate nanotubes and characterize the sorbent using X-ray photoelectron spectroscopy (XPS), (ii) investigate the sorption behavior of titanate nanotubes under different solution compositions, (iii) utilize surface complexation model to fit experimental data and simulate sorption process, and (iv) provide a mechanistic description of the sorption process.

2. Materials and methods

2.1. Chemicals

All chemicals are reagent grade unless otherwise stated. Sodium hydroxide (NaOH) pellets were supplied by VWR BDH. Titanium dioxide (Merck) was used as precursor for the synthesis of sodium

* Corresponding author.
E-mail address: ddsun@ntu.edu.sg (D.D. Sun).

0304-3894/$ – see front matter © 2011 Elsevier B.V. All rights reserved.
doi:10.1016/j.jhazmat.2011.01.053

titanate nanotubes (STN). Synthesis procedure was a modified version of Kasuga et al. [12]. Typically, 4 g of TiO_2 powder was added to 50 mL NaOH solution (10 M). The mixture was stirred for 1 day and loaded into an acid digestion bomb (125 mL, Parr Instruments) for 2 days at 150 °C. As-synthesized STN were retrieved from the Teflon cup and washed with de-ionized (DI) water in a 1 L HDPE bottle. After 1 day, the STN were separated (centrifuged at 10,000 rpm for 30 min) and washed with de-ionized water. The washing process was repeated until solution has neutral pH and a conductivity of 10^{-6} S/cm. The STN were freeze dried and added into de-ionized water to form slurry of known concentration. The slurry was subject to conditioning in an end-over-end mixer for 2 weeks. To ensure a homogenous STN stock the slurry was transferred to a settling column to separate larger aggregates. After 30 min the supernatant in the column was retrieved and the concentration of STN in supernatant was calculated by determining the dry weight of the settled particles. The BET surface area of the STN was 206 m^2/g.

2.2. Equipments

X-ray photoelectron spectroscopy (XPS) analyses were carried out in an ultrahigh vacuum (UHV) chamber with a base pressure below 2.66×10^{-7} Pa at room temperature. Photoemission spectra were recorded by a Kratos Axis Ultra spectrometer equipped with a standard monochromatic Al Kα excitation source ($h\nu$ = 1486.71 eV). The pass energy and step size of low-resolution XPS scan were performed at 160 eV and 1 eV, respectively. For the high-resolution XPS scan, the parameters above were adjusted to 40 eV and 0.1 eV. Due to surface charge effects, the binding energy (BE) scale was calibrated using C 1 s peak at 284.8 eV. Background was corrected with Shirley and peaks were fitted with Gaussian–Lorentzian (GL) function. XPS samples were lightly dust onto a double-sided carbon tape [13]. Cadmium was measured using inductively coupled plasma optical emission spectrophotometer (ICP-OES, Perkin Elmer Optima 2000).

2.3. Experiments

The rationale of choosing nitrate for all chemicals ($Cd(NO_3)_2{\cdot}4H_2O$, HNO_3 and $NaNO_3$) is to ensure interference of anion to sorption is minimal. Nitrate is known to bind weakly to surface of metal oxides [14]. Thereby, most, if not all, sites were made available for Cd-sorption studies. Discontinuous batch titration was conducted in this work [15]. Suspension of 12.5 g/L STN with appropriate ionic strength (IS) was prepared and divided into aliquots of 20 mL. pH were adjusted with 0.25 M HNO_3 and NaOH. The pH value was measure using a Horiba pH meter/electrode. Readings were taken after 5–10 min. Kinetics was performed to determine the duration required to achieve a pseudo-equlibrium. Two 1 L HDPE bottles containing 0.05 g/L STN were adjusted to pH 3 and 4.8. Third bottle of DI water (without STN) were used as a control. At various time intervals 10 mL sample were collected, filtered (0.2 μm Nylon, Sartorius). The filtrates were preserved with 20 μL HNO_3 (70%). Samples were measured for Cd, Na and Ti. Dissolution was not considered in this study as it was found that molarity of Ti at pH 3 was negligible (Fig. S1). Sorption edge and isotherm studies were conducted with samples of 50 mL each containing appropriate proportions of STN and ionic strength. Cadmium was spiked into the solution followed by end-over-end mixing for 24 h. pH values before and after equilibration were recorded. The samples were then subject to centrifuging at 10,000 rpm and 30 min. All samples were filtered prior to analyses. A blank sample (i.e. without STN) was prepared for each set of test as a control. All equilibration were performed in the dark.

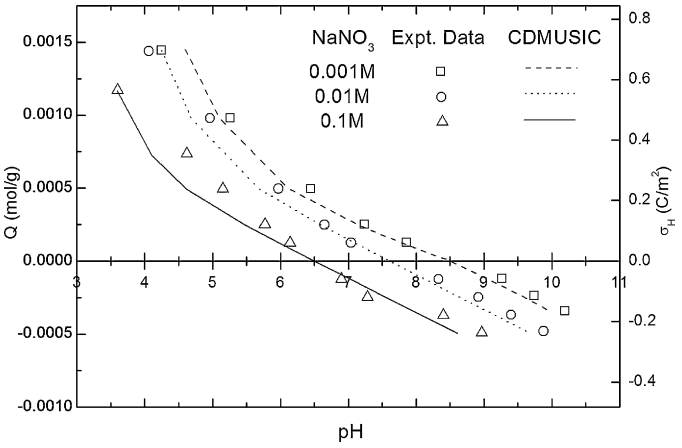

Fig. 1. Titration curves of STN under different ionic strengths. STN = 12.5 g/L; V = 0.02 L.

2.4. Modeling software

In this work, computations involving speciation, titration and sorption were perform using PhreePlot [16]. Thermodynamic constants were from wateq4f.dat database. For the modeling of titration and sorption experiment data a charge distribution multisite ion complexation (CDMUSIC) model was chosen [17]. In comparison with other models CDMUSIC is able to describe sorption at different ionic strength and able to achieve a better fit with its charge distribution function [18,19]. A sample of the programming language used in this work can be found in the supporting information.

3. Results and discussion

3.1. Acid–base titration

Titration was conducted at different ionic strength (IS). It is evident that STN is positively charged at acidic condition and negatively charged at basic condition (Fig. 1). At each IS, a point of zero charge (PZC) can be observed. The curves are parallel and do not intersect and STN is less protonated at higher IS. At IS = 0.1 M, high concentration of Na^+ ion competes with protons for binding sites and, thereby, reduces the amount of protons being sorbed. When pH > PZC, effect of de-protonation is lesser at lower ionic strength. These characteristics of STN titration curves are similar to clays [20]. The shape of titration curves can be explained by the origin of the charges. Titanate nanotube is different from bulk anatase or rutile. The titanate nanotube has a layered structure and two types of charges. At the solid–water interface hydroxyl groups (≡TiOH) are variably-charged and permanently-charged sites ($\equiv Ti_3O_7^{2-}$) are located within the interlayer which is also the walls of the tube.

3.2. Sorption isotherms

In order to elucidate the effect of pH on sorption capacity, isotherm studies were carried out (Fig. 2). Each set of data points was fitted with Langmuir isotherm:

$$q = \frac{q_m K_L C_e}{1 + K_L C_e} \quad (1)$$

where q is the amount of cation sorbed at equilibrium (mol/g), q_m is the sorption capacity of STN, K_L is Langmuir sorption constant (L/mol) and C_e is the concentration of solution cation at equilibrium (mol/L). It is observed that increasing Cd concentration resulted in increase of Cd uptake until a saturation point. Subsequent increase

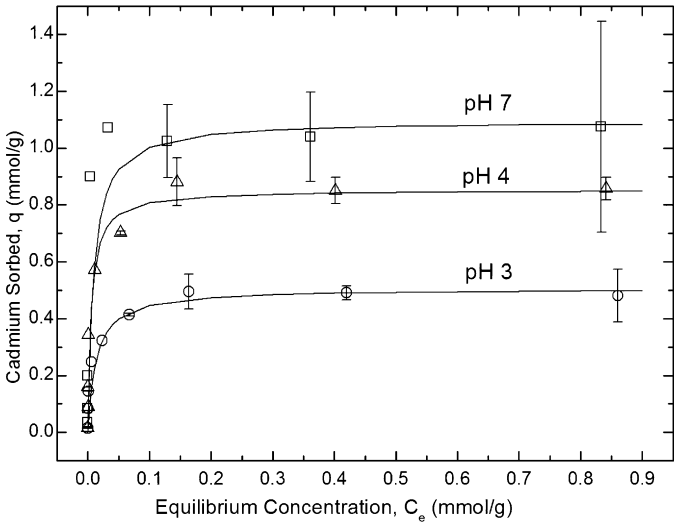

Fig. 2. Sorption isotherms of Cd on STN. Scale bars represent standard deviation of triplicates. Lines are Langmuir isotherms. STN = 0.05 g/L; $NaNO_3$ = 0.1 M.

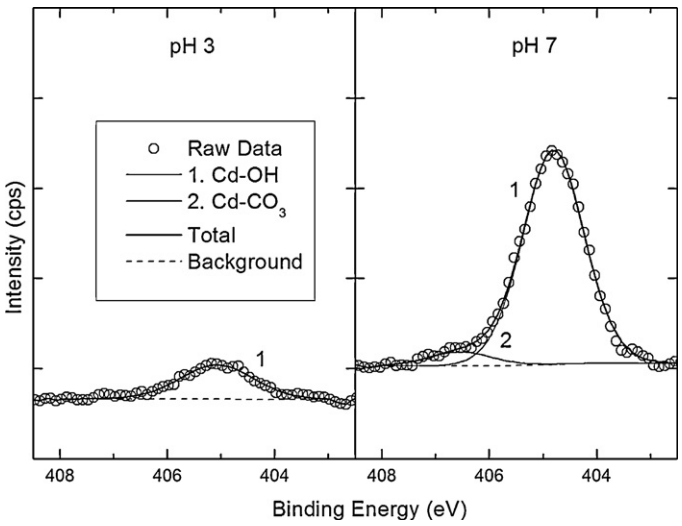

Fig. 3. Deconvolution of $Cd_{5/2}$ peaks of Cd-sorbed STN at different pH conditions. STN = 0.05 g/L; $NaNO_3$ = 0.1 M; $Cd_{initial}$ = 10^{-4} M.

of Cd concentration only resulted in a plateau. This indicates Cd ions has fully occupied and saturated the possible sites on STN. At pH 3 sorption capacity is only half of that at pH 7 thus, the sorption capacity is largely affected by solution pH. Nevertheless, sorption capacity (q_m) at neutral pH was 1.1 mmol/g which is higher than other metal oxides and clays reported [21,22]. The mechanisms behind this relatively higher sorption capacity of STN will be discussed in the following sections.

3.3. X-ray photoelectron spectroscopy

Due to the detection limit of XPS, the concentrations of STN and Cd were higher than that of batch tests. The ratio of sorbent to sorbate remains the same as batch tests. Increased concentrations did not affect the shape of sorption edge. It is known that valence state of cadmium in aqueous is +2 [1,23]. XPS is performed on samples after equilibration at pH 3 and 7. The data indicated an increasing surface Cd with increasing pH (Fig. S2). At pH 3, Cd $3d_{5/2}$ and Cd $3d_{3/2}$ peaks were found at 405.4 eV and 412.1 eV respectively. Under neutral and basic conditions, the peaks shifted to lower binding energy. Peaks of Cd $3d_{5/2}$ and Cd $3d_{3/2}$ were shifted to 405.0 eV and 411.6 eV, respectively. This is attributed to the presence of two types of Cd bond present on STN at pH 7. This can be explained by the deconvolution of Cd $3d_{5/2}$ peaks as shown in Fig. 3.

It reveals there a primary curve for pH 3 whereas two primary curves for pH 7. Curve 1 corresponds to Cd–O bond in which oxygen originates from the surface hydroxyl groups of STN rather than the solution species, $CdOH^+$. As shown from the speciation curves (Fig. S5), at pH 7, cadmium is present as Cd^{2+} rather than $CdOH^+$. Curve 2 is attributed to the presence of $CdCO_{3(s)}$, otavite. It is known that Cd–CO_3 bond has a higher binding energy position than Cd–O [13]. Note that at a higher $Cd_{initial}$ precipitation of otavite shifts to pH 7 as shown from the speciation curve. Hence, it is expected that Cd will precipitate as $CdCO_{3(s)}$ for sorption at pH 7. Table S1 quantifies the raw areas of all the Cd peaks and it is observed that the areas of both Curve 1 and 2 increases as pH increase.

The presence of $CdCO_{3(s)}$ on sample pH 7, in theory, should be reflected in C 1s spectrum and this would give a quantitative confirmation of the presence of precipitation. This method, however, is not practical due to the strong signals from adventitious carbon and the adhesive carbon tape. Any possible signals from the low concentration of $CdCO_{3(s)}$ would be overlapped by the other two carbon sources. Fig. S3 showed that all peaks have same binding energy positions suggesting the signals originate from the same dominant source (i.e. carbon tape).

In order to verify the presence of ion-exchange process involved, XPS scans were done on Na 1s. High resolution scan of Na 1s peaks (Fig. 4) reveal that Na was absent from the sample which undergone sorption at pH 3. This could be explained by the exchange of protons with Na ions within STN interlayer to form hydrogen titanate. However, at pH 7 the peak area was also reduced when compared to peaks before sorption. With a higher fractional uptake of Cd at these pH conditions, Na ions are being exchanged by Cd ions during the sorption process.

3.4. Sorption kinetics

Kinetic studies were conducted to determine whether Na^+ has been released during the sorption process. Concentration of STN was in excess to ensure the sufficient sites were available for Cd bonding. From Fig. 5, Cd was not detected in solution after 10 min at pH 4.8. In contrast, maximum Cd sorption efficiency at pH 3 was only 80%.

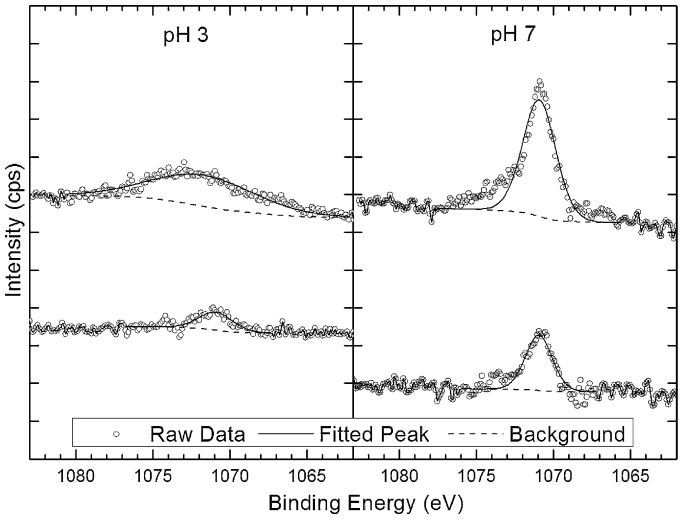

Fig. 4. Na 1 s peaks of samples before (top curve) and after (bottom) sorption under different pH conditions. STN = 0.05 g/L; $NaNO_3$ = 0.1 M; $Cd_{initial}$ = 10^{-4} M.

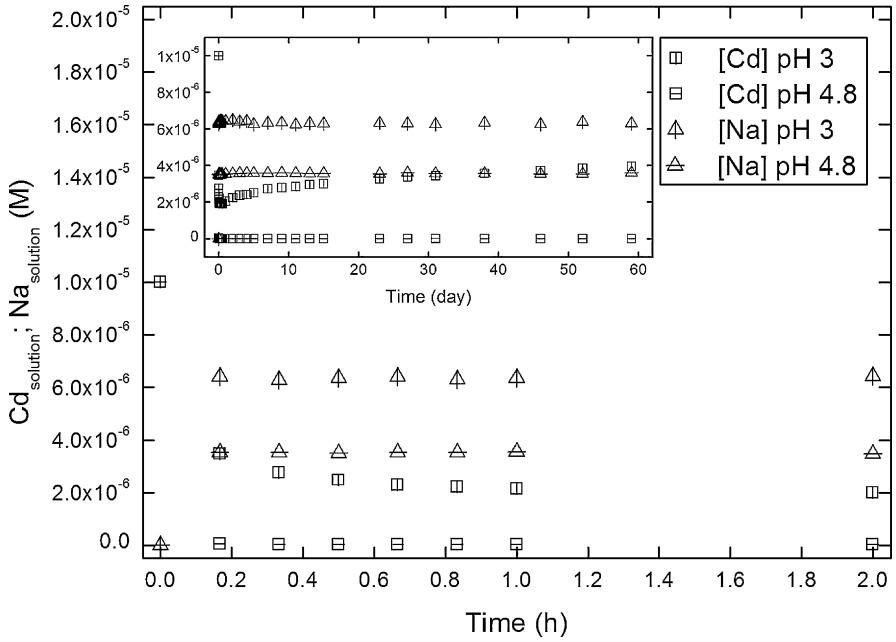

Fig. 5. Kinetic studies of Cd and Na at pH 3 and 4.8. STN = 0.05 g/L; $Cd_{initial} = 10^{-5}$ M.

Pseudo-second-order rate model was fitted to the sorption data (Fig. S4 main). It was found that, at pH 3, Cd sorption can be described by the pseudo-second-order equation. This model is known to encompass the reactions of external film diffusion, surface adsorption and intra-particle diffusion [24]. The rate-limiting step is the putative solute diffusion into the bulk sorbent. Firstly, Cd ions can diffuse and adsorb onto outer wall of STN relatively quickly. Upon the saturation of outer sites, the slower reactions would be the diffusion of cations into the interlayers and the mass transfer to the inner wall of the tube. Despite the good linear regression analysis (Fig. S4 inset), the model was unable to fit sorption kinetics at pH 4.8. The reason for this incompatibility could be due to the faster kinetics and different sorption mechanism. Reaction rate models are known to have their inadequacy in modeling sorption data. Regardless of the orders of reaction, these models are affected by only apparent parameters (e.g. initial concentration, sorbent dosage and type of solute) and failed to consider other equally pertinent conditions [25]. In this case, the difference due to effect of pH cannot be simulated using the pseudo-second-order equation.

Prolonged mixing over at pH 3 resulted in desorption of Cd. It was observed that after Day 1, Cd in solution increased gradually and equilibrium was not achieved during the 60 day test. At pH 3 more protons compete with cadmium ions for high energy sites on STN. During the 60 days there is shifting of cadmium ions from high energy sites to low energy sites and to the bulk solution. The trend is not uncommon and has been reported in other works. It has been pointed out that, at a given pH, contact time affects the sorption efficiency [26]. In this study, Cd was desorbed from STN due to the high concentration of protons in the solution. Nevertheless, equilibration duration of 24 h was chosen for subsequent batch test studies. In a sorption process involving only ion-exchange the uptake of Cd^{2+} should release a stoichiometrically-equivalent amount of Na^+ as shown in Eq. (2) (i.e. for every 1 Cd^{2+} ion, 2 Na^+ ions should be released):

$$Na_2X + Cd^{2+} \rightarrow CdX + 2Na^+ \quad (2)$$

where X^{2-} represents $\equiv Ti_3O_7{}^{2-}$, the fixed charge at the interlayer of nanotube. In this study, however, concentrations of Na^+ measured is much less than the theoretical amount calculated from Eq. (2). Hence sorption of Cd should not involve purely ion-exchange mechanism. It is indeed plausible that fresh STN is already in the form of $H_xNa_{2-x}Ti_3O_7$ at low solution pH. Under acidic condition exchange of Cd^{2+} with protons is possible.

3.5. Effect of ionic strength

Ionic strength was varied to investigate its effect of on sorption efficiency (Fig. 6). Percentage of Cd being sorbed by STN was calculated by:

$$Cd_{sorbed}(\%) = \frac{C_o - C_e}{C_e} \times 100\% \quad (3)$$

where C_o and C_e are the initial and equilibrium cadmium concentration (M). About 90% of cadmium ions were sorbed at pH 7.5 before the onset of otavite precipitation, indicating only dissolved cadmium ions are sorbed in the process. Cadmium uptake is higher at basic pH than acidic pH. From the titration of STN we know that the points of zero charge range from 6.5 to 8.5. At pH > PZC, the hydroxyl groups are mainly negatively charged. Negatively charged surface hydroxyl groups are able to sorbed cadmium ion more readily than a positively charged group. It was observed that change in IS did not affect the position of sorption edges significantly from IS = 0.001–0.01 M. Sorption edges which are independent of IS are characteristic of inner-sphere complex formation. In addition, the presence of inner-sphere complexation can also be observed from the acid–base titration plot of the used sorbent. PZC of inner-sphere-complexed sorbent is lower than the virgin sorbent [27]. Cadmium ions are directly bonded onto the surface functional groups rather than being bonded as a hydrated form. This can be explained by the nature of the sorbate. In contrast to ions of alkaline earth metals, cadmium is a soft acid and is able to bond strongly onto metal oxides [1,14,28]. Ions can bond onto the surface regardless of the thickness of the electric double layer. This observation of cadmium ion is in accordance with previous studies on other metal oxides [29,30].

When IS = 0.1 M, however, there was a slight reduction in Cd uptake, indicating that there is more than one sorption mechanism involved, plausibly inner-sphere complexation and ion-exchange. In this study, to determine the bonding mechanisms based on the

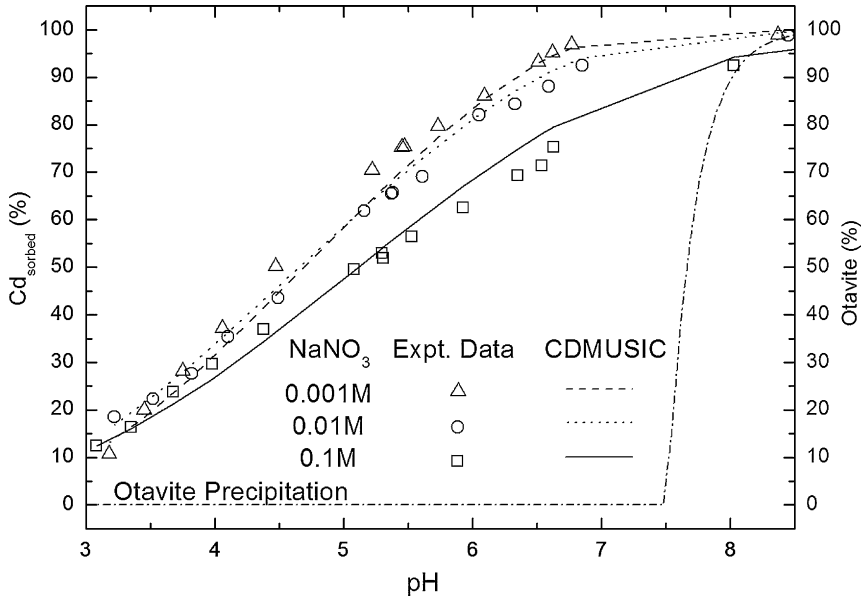

Fig. 6. Effect of IS on Cd uptake as function of pH. STN = 0.005 g/L; $Cd_{initial} = 10^{-5}$ M.

sorption edge gradient is more complex as there are fixed charge in addition to the variably-charged surface sites. Rather, the bonding of Cd ions to STN–water interface is determined by selecting the model which best fits the experimental data.

3.6. Surface complexation modeling

CDMUSIC was used to fit experimental data from titration and sorption tests. The basal plane of the nanotube is the solid–water interface and its singly and doubly coordinated oxygen atoms were identified as potential sites for ion complexation. From crystallographic calculation the density of each site is 2.9 nm^{-2}. In addition the ion-exchange can occur at the interlayer of basal planes and cation exchange capacity from crystallographic calculation is 6.629 meq/g. The capacitances of inner and outer Stern layers were fixed at 0.9 F/m^2 [17]. A two-step fitting approach was used to determine equilibrium constants and Table 1 shows the equations and respective parameters from the final models. Firstly, a titration model is set up to determine affinity constants for Reactions 1–6, 8. Results from titration fitting were input into a second file which involves fitting of sorption edges data to obtain parameters of Reactions 7 and 9.

Both singly and doubly coordinated functional groups are responsible for the acid–base behavior of the nanotubes whereas the triply coordinated group is inert within the pH range of interest and will not be considered in this work [31,32]. For sorption of cadmium ions only singly coordinated oxygen is involved. In our study we found that cadmium adsorption is better described as bidentate instead of monodentate reaction. This is in accordance with previous literature on cadmium sorption [33]. The presence of outer-sphere complexation at the surface is not possible because as stated earlier cadmium is a soft acid and tends to bond strongly to metal oxides [1,14,28]. Addition of outer-sphere reaction (Eq. (4)) did not achieve a better fit than that of inner-sphere reaction alone.

$$2 \equiv TiOH^{0.333-} + Cd^{2+} + H_2O \leftrightarrow (\equiv TiOH)_2CdOH^{0.334+} + H^+ \quad (4)$$

In general better fit was achieved when both surface adsorption and ion-exchange of cadmium ion (Table 1 Reaction 7 and 9) was considered simultaneously. From the results of this work sorption of Cd onto STN involved two mechanisms. Firstly, Cd ions can be adsorbed onto hydroxyl groups at titanate nanotube surface forming inner-sphere complex with the OH groups. Secondly, the heavy metal can be sorbed by ion-exchange at the interlayer. An uptake

Table 1
Equilibrium constants used in CDMUSIC model.

Reaction	Proton[a]	Log K	Δz_0	Δz_1
1	$\equiv Ti_2O^{0.667-} + H^+ \leftrightarrow \equiv Ti_2OH^{0.333+}$	5.14	1[e]	0[e]
2	$\equiv TiOH^{0.333-} + H^+ \leftrightarrow \equiv TiOH_2^{0.667+}$	5.70	1[e]	0[e]
	Electrolyte			
3	$\equiv TiOH^{0.333-} + Na^+ \leftrightarrow \equiv TiOHNa^{0.667+}$	2.21	0[e]	1[e]
4	$\equiv TiOH^{0.333-} + H^+ + NO_3^- \leftrightarrow \equiv TiOH_2NO_3^{0.333-}$	6.60	1[e]	−1[e]
5	$\equiv Ti_2O^{0.667-} + Na^+ \leftrightarrow \equiv Ti_2ONa^{0.333+}$	2.21	0[e]	1[e]
6	$\equiv Ti_2O^{0.667-} + H^+ + NO_3^- \leftrightarrow \equiv Ti_2OHNO_3^{0.667-}$	6.60	1[e]	−1[e]
	Cadmium ion			
7	$2\equiv TiOH^{0.333-} + Cd^{2+} \leftrightarrow (\equiv TiOH)_2Cd^{1.334+}$	9.1	0.3	1.7
	Ion-exchange site[c]			
8	$NaX + H^+ \leftrightarrow Na^+ + HX$	1.4	–	–
9	$2NaX + Cd^{2+} \leftrightarrow 2Na^+ + CdX_2$	−2	–	–

[a] Site densities of singly coordinate sites ($\equiv TiOH^{0.333-}$) = doubly coordinate sites ($\equiv Ti_2O^{0.667-}$) = 2.88 nm^{-1}.
[b] Both capacitances of inner (C_1) and outer (C_2) Stern layer are 0.9 F/m^2.
[c] In the chemical equations ion-exchange site ($\equiv Ti_3O_7^{2-}$) is denoted by X. Cation exchange capacity is calculated to be 6.629 meq/g.
[d] Surface area from BET measurement is 206 m^2/g.
[e] Fixed parameters.

of a single Cd ion results in the release of two monovalent ions into the solution.

4. Conclusion

Titanate nanotubes was synthesized by hydrothermal and applied to remove cadmium. Sorption isotherms showed that titanate nanotubes have high sorption capacity for cadmium (1.1 mmol/g). Low ionic strength (<0.01 M) did not have significant effect on the sorption behavior, indicating cadmium formed inner-sphere complexation onto titanate surface. XPS data revealed decrease in surface Na after sorption equilibrium suggesting an underlying ion-exchange mechanism. On top of spectroscopic result, CDMUSIC modeling based on inner-sphere complexation and ion-exchange mechanism fitted the experimental data. Thereby sorption of cadmium onto titanate nanotubes can be ascribed to (i) complexation at the surface hydroxyl and (ii) ion-exchange at the inter-layers of the basal plane.

Acknowledgements

A.J.D. is grateful to David G. Kinniburgh for help on PhreePlot. Discussions with Xiwang Zhang are greatly appreciated. Comments and feedbacks from anonymous reviewers have greatly improved the quality of the manuscript. This research work was supported by Singapore Environment & Water Industry (EWI) Development Council (MEWR 621/06/166).

Appendix A. Supplementary data

Supplementary data associated with this article can be found, in the online version, at doi:10.1016/j.jhazmat.2011.01.053.

References

[1] H.S. Posselt, W.J. Weber, Environmental Chemistry of Cadmium in Aqueous Systems, University of Michigan, Dept. of Civil Engineering, 1971, p. 178.
[2] M. Kasuya, Recent epidemiological studies on itai-itai disease as a chronic cadmium poisoning in Japan, Water Science and Technology 42 (2000) 147–154.
[3] S. Satarug, M.R. Moore, Adverse health effects of chronic exposure to low-level cadmium in foodstuffs and cigarette smoke, Environmental Health Perspectives 112 (2004) 1099–1103.
[4] C. Gerente, V.K.C. Lee, P.L. Cloirec, G. McKay, Application of chitosan for the removal of metals From wastewaters by adsorption—mechanisms and models review, Critical Reviews in Environmental Science and Technology 37 (2007) 41–127.
[5] Z. Reddad, C. Gerente, Y. Andres, P. Le Cloirec, Adsorption of several metal ions onto a low-cost biosorbent: kinetic and equilibrium studies, Environmental Science & Technology 36 (2002) 2067–2073.
[6] S.E. Bailey, T.J. Olin, R.M. Bricka, D.D. Adrian, A review of potentially low-cost sorbents for heavy metals, Water Research 33 (1999) 2469–2479.
[7] X. Zhang, J.H. Pan, A.J. Du, W. Fu, D.D. Sun, J.O. Leckie, Combination of one-dimensional TiO_2 nanowire photocatalytic oxidation with microfiltration for water treatment, Water Research 43 (2009) 1179–1186.
[8] X. Sun, Y. Li, Synthesis and characterization of ion-exchangeable titanate nanotubes, Chemistry-A European Journal 9 (2003) 2229–2238.
[9] H.H. Ou, C.H. Liao, Y.H. Liou, J.H. Hong, S.L. Lo, Photocatalytic oxidation of aqueous ammonia over microwave-induced titanate nanotubes, Environmental Science & Technology 42 (2008) 4507–4512.
[10] H.Y. Niu, J.M. Wang, Y.L. Shi, Y.Q. Cai, F.S. Wei, Adsorption behavior of arsenic onto protonated titanate nanotubes prepared via hydrothermal method, Microporous Mesoporous Materials 122 (2009) 28–35.
[11] S.-S. Liu, C.-K. Lee, H.-C. Chen, C.-C. Wang, L.-C. Juang, Application of titanate nanotubes for Cu(II) ions adsorptive removal from aqueous solution, Chemical Engineering Journal 147 (2009) 188–193.
[12] T. Kasuga, M. Hiramatsu, A. Hoson, T. Sekino, K. Niihara, Formation of titanium oxide nanotube, Langmuir 14 (1998) 3160–3163.
[13] J.F. Moulder, Handbook of X-Ray Photoelectron Spectroscopy: A Reference Book of Standard Spectra for Identification and Interpretation of XPS Data, Physical Electronics, Eden Prairie, MN, 1995.
[14] K.F. Hayes, Equilibrium, Spectroscopic and Kinetic Studies of Ion Adsorption At The Oxide/Aqueous Interface, Stanford University, 1987.
[15] L. Sigg, W. Stumm, The interaction of anions and weak acids with the hydrous goethite surface, Colloid and Surface 2 (1981) 101–117.
[16] D.G. Kinniburgh, D.M. Cooper, PhreePlot – Creating graphical output with PHREEQC, 2009.
[17] T. Hiemstra, W.H. Van Riemsdijk, On the relationship between charge distribution, surface hydration, and the structure of the interface of metal hydroxides, Journal of Colloid and Interface Science 301 (2006) 1–18.
[18] C.A.J. Appelo, M.J.J. Van Der Weiden, C. Tournassat, L. Charlet, Surface complexation of ferrous iron and carbonate on ferrihydrite and the mobilization of arsenic, Environmental Science & Technology 36 (2002) 3096–3103.
[19] M. Villalobos, M.A. Trotz, J.O. Leckie, Surface complexation modeling of carbonate effects on the adsorption of Cr(VI), Pb(II), and U(VI) on goethite, Environmental Science & Technology 35 (2001) 3849–3856.
[20] A.M.L. Kraepiel, K. Keller, F.M.M. Morel, On the acid–base chemistry of permanently charged minerals, Environmental Science & Technology 33 (1998) 516–1516.
[21] Y. Gao, R. Wahi, A.T. Kan, J.C. Falkner, V.L. Colvin, M.B. Tomson, Adsorption of cadmium on anatase nanoparticles effect of crystal size and pH, Langmuir 20 (2004) 9585–9593.
[22] S.S. Gupta, K.G. Bhattacharyya, Removal of Cd(II) from aqueous solution by kaolinite, montmorillonite and their poly(oxo zirconium) and tetrabutylammonium derivatives, Journal of Hazardous Materials 128 (2006) 247–257.
[23] C.F. Baes, R.E. Mesmer, The Hydrolysis of Cations, Wiley, New York, 1976.
[24] X.E. Shen, X.Q. Shan, D.M. Dong, X.Y. Hua, G. Owens, Kinetics and thermodynamics of sorption of nitroaromatic compounds to as-grown and oxidized multiwalled carbon nanotubes, Journal of Colloid and Interface Science 330 (2009) 1–8.
[25] Y.S. Ho, G. McKay, The kinetics of sorption of divalent metal ions onto sphagnum moss peat, Water Research 34 (2000) 735–742.
[26] D.L. Sparks, Metal and oxyanion sorption on naturally occurring oxide and clay mineral surfaces, in: V.H. Grassian (Ed.), Environmental Catalysis, Taylor & Francis Group, Boca Raton, FL, 2005.
[27] H. Hohl, L. Sigg, W. Stumm, Characterization of surface chemical properties of oxides in natural waters, in: M.C. Kavanaugh, J.O. Leckie (Eds.), Particulates in Water, American Chemical Society, 1980, pp. 1–31.
[28] C. Papelis, Cadmium and Selenite Adsorption on Porous Alumium Oxides: Equilibrium, Rate of Uptake, and Spectroscopic Studies, Stanford University, 1992.
[29] C. Papelis, G.E. Brown, G.A. Parks, J.O. Leckie, X-ray absorption spectroscopic studies of cadmium and selenite adsorption on aluminum oxides, Langmuir 11 (2002) 2041–2048.
[30] K.F. Hayes, J.O. Leckie, Modeling ionic strength effects on cation adsorption at hydrous oxide/solution interfaces, Journal of Colloid and Interface Science 115 (1987) 564–572.
[31] T. Hiemstra, W.H. Van Riemsdijk, G.H. Bolt, Multisite proton adsorption modeling at the solid/solution interface of (hydr)oxides: a new approach: I model description and evaluation of intrinsic reaction constants, Journal of Colloid and Interface Science 133 (1989) 91–104.
[32] K. Bourikas, T. Hiemstra, W.H. Van Riemsdijk, Ion pair formation and primary charging behavior of titanium oxide (anatase and rutile), Langmuir 17 (2001) 749–756.
[33] P. Venema, T. Hiemstra, W.H. Van Riemsdijk, Multisite adsorption of cadmium on goethite, Journal of Colloid and Interface Science 183 (1996) 515–527.